New Reference Materials and Assessment of Matrix Effects for SIMS Measurements of Oxygen Isotopes in Garnet

Alice **Vho** (1)*, Daniela **Rubatto** (1, 2), Benita **Putlitz** (2) and Anne-Sophie **Bouvier** (2)

(1) Institute of Geological Sciences, University of Bern, Bern, CH-3012, Switzerland
(2) Institute of Earth Sciences, University of Lausanne, Lausanne, CH-1015, Switzerland
* Corresponding author. e-mail: alice.vho@geo.unibe.ch

Abstract

Accurate ion microprobe analysis of oxygen isotope ratios in garnet requires appropriate reference materials to correct for instrumental mass fractionation that partly depends on the garnet chemistry (matrix effect). The matrix effect correlated with grossular, spessartine and andradite components was characterised for the Cameca IMS 1280HR at the SwissSIMS laboratory based on seventeen reference garnet samples. The correlations fit a second-degree polynomial with maximum bias of *ca*. 4‰, 2‰ and 8‰ respectively. While the grossular composition range 0–25% is adequately covered by available reference materials, there is a paucity of them for intermediate compositions. We characterise three new garnet reference materials GRS2, GRS-JH2 and CAP02 with a grossular content of 88.3 ± 1.2% (2*s*), 83.3 ± 0.8% and 32.5 ± 3.0% respectively. Their micro scale homogeneity in oxygen isotope composition was evaluated by multiple SIMS sessions. The reference $\delta^{18}O$ value was determined by CO_2 laser fluorination ($\delta^{18}O_{LF}$). GRS2 has $\delta^{18}O_{LF}$ = 8.01 ± 0.10‰ (2*s*) and repeatability within each SIMS session of 0.30–0.60‰ (2*s*), GRS-JH2 has $\delta^{18}O_{LF}$ = 18.70 ± 0.08‰ and repeatability of 0.24–0.42‰ and CAP02 has $\delta^{18}O_{LF}$ = 4.64 ± 0.16‰ and repeatability of 0.40–0.46‰.

Keywords: oxygen isotopes, SIMS, ion microprobe, reference materials, garnet.

Received 28 Nov 19 – Accepted 06 Mar 20

This article has been accepted for publication and undergone full peer review but has not been through the copyediting, typesetting, pagination and proofreading process, which may lead to differences between this version and the Version of Record. Please cite this article as doi: 10.1111/GGR.12324

Significant advances in stable isotope analyses by secondary ion mass spectrometer (SIMS) in the last decades have led to an improvement in precision (down to ± 0.1–0.3‰, 2*s*) and spatial resolution (down to < 10 µm) (e.g., Eiler *et al.* 1997, Riciputi *et al.* 1998, Kita *et al.* 2009, Ickert and Stern 2013, Martin *et al.* 2014, Regier *et al.* 2018). The great advantage of this in situ technique is the capability of resolving variations within single mineral grains and analysing fine-grained minerals with preservation of textural information. The principal limitation remains the instrumental mass fractionation dependent upon sample chemistry, termed the matrix effect (Eiler *et al.* 1997). Thus accuracy strongly relies on reference materials that are as close as possible to the chemistry of the unknowns.

Garnet is a key mineral used in metamorphic petrology to constrain pressure, temperature and time paths. It commonly records different stages of the rock evolution as distinct mineral zones, which oxygen isotope compositions may assist to reconstruct fluid-rock interaction and fluid sources over the metamorphic evolution of the host rock (e.g., Chamberlain and Conrad 1991, Errico *et al.* 2013, Page *et al.* 2013, Martin *et al.* 2014, Rubatto and Angiboust 2015, Quinn *et al.* 2017). Garnet is a solid solution between five main end-members: grossular (Grs, $Ca_3Al_2Si_3O_{12}$), pyrope (Prp, $Mg_3Al_2Si_3O_{12}$), almandine (Alm, $Fe_3Al_2Si_3O_{12}$), spessartine (Sps, $Mn_3Al_2Si_3O_{12}$) and andradite (And, $Ca_3Fe^{3+}{}_2Si_3O_{12}$). It has been demonstrated that grossular, andradite and spessartine components can be correlated with significant mass fractionation (Vielzeuf *et al.* 2005a, Page *et al.* 2010, Ickert and Stern 2013, Martin *et al.* 2014). In this study, we present an empirical model that relates mass bias to grossular, andradite and spessartine abundance in garnet for the Cameca IMS 1280HR at the SwissSIMS laboratory (University of Lausanne). We additionally consider the variation of this scheme over time and compare it with results from previous studies.

To adequately quantify the matrix effect for minerals with complex chemistry as garnet, an extensive suite of reference materials covering a wide compositional range is required (Page *et al.* 2010, Raimondo *et al.* 2012, Ickert and Stern 2013, Martin *et al.* 2014). Along the grossular compositional range, previously characterised reference

materials have composition mostly between Grs = 0–25% and a few of them in the range Grs = 85–95% (Page *et al.* 2010, Martin *et al.* 2014). Such high-grossular compositions are typical for thermally and regionally metamorphosed impure calcareous rocks, rocks that have undergone calcium metasomatism (e.g., rodingites) and metamorphosed Ca-rich basalts (Deer *et al.* 1992). To supplement the available reference materials and improve the accuracy of the correction for high and intermediate grossular compositions, new garnet samples GRS2, GRS-JH2 and CAP02 suitable as reference materials for SIMS oxygen isotope analysis are introduced in this study.

Reference materials used for matrix effect evaluation

To perform accurate matrix corrections for oxygen isotope measurements in garnet, thirteen previously investigated garnet reference materials and three newly characterised garnet samples were used in this study to cover a large range in grossular, andradite and spessartine compositional space (Figure 1). To cover the grossular compositional range, reference materials UWG2 (Valley *et al.* 1995), 10691 (Kohn and Valley 1998, Page *et al.* 2010), B114, PRP-AA, PRP-AK, 2B3 (Vielzeuf *et al.* 2005a, b), Kakanui (Gonzaga *et al.* 2010, Urosevic *et al.* 2018), as well as GRS2 , GRS-JH2 and CAP02 (this study) were analysed. To cover the spessartine compositional range, reference materials were UWG2 (Valley *et al.* 1995), 2B3 (Vielzeuf *et al.* 2005a,b), SPEBH, GRT1A (Martin *et al.* 2014) and ErrRED (Urosevic *et al.* 2018). Reference materials to cover the grossular–andradite join were LEW10, LEW6, 92-W2, 10691 (Kohn and Valley 1998, Page *et al.* 2010), 2B3 (Vielzeuf *et al.* 2005a,b) and AndRG (Martin *et al.* 2014).

Garnet crystals GRS2 and GRS-JH2 were bought at a mineral fair and their likely provenance is Afghanistan. GRS2 is a crystal of ~ 0.4 g light brown in colour, GRS-JH2 is a crystal of ~ 1.4 g dark orange-brown in colour. CAP02 is a light pink garnet separated from an eclogite found in the mafic-ultramafic lens of Capoli in the Central Swiss Alps (Brouwer *et al.* 2005). Garnet constitutes *ca*. 70% of the sample that also contains omphacite and accessory rutile.

Analytical methods

Sample preparation

Previously characterised garnet reference materials were crushed by hand, cast in three epoxy disks with diameter of 25 mm, each one containing multiple grains or grain fragments of the available reference materials for the grossular, andradite and spessartine compositional ranges. These three mounts are referred to as GRT-GRS, GRT-AND and GRT-SPS respectively. Fragments of garnet crystals GRS-JH2 and GRS2 were mounted in GRT-GRS together with previously characterised reference materials. Each mount contains several grains of UWG2 to be used as internal reference material. The samples were located in the central 10 mm of the mount to avoid possible sample location effects (Peres *et al.* 2013).

CAP02 sample was disaggregated using a Selfrag apparatus at the Institute of Geological Sciences, University of Bern, which produced a high yield of intact mineral grains by high-voltage pulsing, and sieved to select the grain fraction between 125 and 500 µm. Around forty inclusion-free garnet crystals of 150–250 µm size were hand-picked and mounted in a epoxy disks with a diameter of 25 mm, together with multiple grains of UWG2 as an 'internal' reference material and a few fragments of the garnet GRS-JH2. The samples were located in the central 10 mm of the mount to avoid possible sample location effects (Peres *et al.* 2013).

All the epoxy mounts were ground to expose the grains and then polished with 6, 3 and 1 µm diamond paste. The topography of the mounts was checked with a light microscope and was less than 5 µm in all cases. All the mounts were carefully cleaned and coated with gold prior to SIMS analysis. The mount containing CAP02 and the mount GRT-GRS containing GRS2 and GRS-JH2 were subsequently polished to remove the gold coating and coated with carbon prior to EPMA analysis.

Electron probe microanalysis

Major element composition of the garnet CAP02, GRS2 and GRS-JH2 was determined by electron probe microanalysis (EPMA) using a JEOL JXA-8200 superprobe at the Institute of Geological Sciences, University of Bern. Garnet was analysed in point beam mode with

an accelerating potential of 15 kV and 20 nA beam current. The counting time was 20 s on peak and 10 s off-peak. For the calculation of mineral formulae from chemical analyses, almandine, pyrope, grossular, spessartine, andradite and Ca-Ti garnet end-members were taken into consideration. Fe^{2+}/Fe^{3+} was estimated by charge balance, assuming no site vacancies or OH substitution. Mineral stoichiometry was determined by normalising to twelve oxygens (formula calculation from the Excel spreadsheet Mineral Normalization v.16, John Brady, Smith College and Dexter Perkins, University of North Dakota, https://serc.carleton.edu/research_education/equilibria/mineralformulaerecalculation.html). Results are reported in Table 1.

Oxygen isotope composition by CO_2 laser fluorination

Oxygen isotope compositions of GSR2, GRS-JH2 and CAP02 were determined at the stable isotope laboratory of the University of Lausanne using the CO_2-laser fluorination technique. The analyses followed the method initially described by Sharp (1990); the details on the procedure in Lausanne are reported by Lacroix and Vennemann (2015). During each measurement session, garnet aliquots in form of small chips of about 1.5–2.5 mg were measured together with the NBS-28 quartz reference material (accepted value 9.64‰, Coplen *et al.* 1983). The garnet data were corrected to the session value of the NBS-28 quartz and given in conventional δ-notation, relative to Vienna Standard Mean Ocean Water (VSMOW). The accuracy and uncertainty of NBS-28 quartz and the repeatability of the garnet analysis are reported in Table 2.

***In situ* analysis of oxygen isotopes by SIMS**

$^{18}O/^{16}O$ ratios were measured using the SwissSIMS Cameca IMS 1280HR instrument at University of Lausanne (Switzerland). Analytical conditions followed Seitz *et al.* (2017). A 10 kV $^{133}Cs^+$ primary Gaussian beam was used with a 1.6–2.1 nA current. This resulted in a typical spot size of 15–25 µm. The electron flood gun was used to compensate surface charge. The energy slit was 50 eV and secondary ion intensities for ^{16}O were typically 1.5–1.7 × 10^9 cps. One session (GRT-SPS mount, August 2016) had count rates of 2.1–2.2 × 10^9 cps. A pre-analysis sputtering time of 30 s was applied to remove the gold coating, followed by automated secondary beam centring and twenty cycles of 5 s data acquisition. Oxygen isotope ratios ($^{18}O/^{16}O$) are in delta notation ($\delta^{18}O$ in ‰) relative to

the Vienna Standard Mean Ocean Water (VSMOW). Raw data tables for each session are given in the online supporting information Appendix S1.

In order to investigate the stability of the matrix effect on the long term, the measurement sessions were distributed over a time window of more than three years. This allows possible effects associated with instrument tuning – performed before each session – to be detected. The mount GRT-GRS was analysed during three sessions (April 2016, December 2016, October 2018), the mount GRT-SPS during 4 sessions (August 2016, August 2017, July 2018, October 2018) and the mount GRT-AND during two sessions (March 2017, June 2019) (Table 3). Each mount was measured during one additional session (August 2016 for GRT-GRS, December 2016 for GRT-SPS, December 2016 for GRT-AND) during which UWG2 and two other reference materials of different composition were analysed (GRS2 and GRS-JH2 in GRT-GRS, 2B3 and ErrRED in GRT-SPS, 2B3 and 10691 in GRT-AND). These latter measurements were not used to calibrate the matrix correction curves, but they were used as independent data to validate the calculated functions. UWG2 was measured as primary reference material to monitor the instrument stability and to correct for the matrix-independent instrumental mass fractionation (IMF). UWG2 analyses bracketed the analyses on other materials and were homogenously distributed over the session with a proportion of 1 to 3. Data for the evaluation of the oxygen isotope homogeneity of garnet GRS2 and garnet GRS-JH2 were extracted from the mount GRT-GRS measurement sessions, for a total of seventy-nine spot analyses on five grain fragments for GRS2 and seventy-one spot analyses on six grain fragments for GRS-JH2 (Figure 2). The standard error on the measurements or 'internal error', also referred to as 'within-spot uncertainty' by Ickert and Stern (2013), is the uncertainty on the mean value of the isotope ratios measured during a single-spot analysis. In the Cameca software, this value corresponds to the standard deviation of the mean (= standard error) of the twenty isotope ratios measured during a single-spot measurement (i.e., twenty cycles of 5 s each, see above). The measured standard errors range between 0.10‰ and 0.47‰ (2SE). An instrumental drift correction was performed only for one session (April 2016) using a linear relation with time based on the linear interpolation of the measurements on the reference material UWG2; no time-related drift occurred during the other sessions.

Data for CAP02 were obtained during three sessions (March 2018, October 2018, June 2019) for a total of sixty-five spot analyses on twenty-five different grains (Figure 2). One analysis of the primary reference material UWG2 was measured every three to four analyses of CAP02 and one analysis of GRS-JH2 every three to six analyses of CAP02 to monitor the instrument stability. The standard error on the measurements ranges between 0.11‰ and 0.26‰ (2SE).

The estimation and correction of the total instrumental mass fractionation during oxygen isotope measurements in garnet reference materials follows the two-step procedure described in Page *et al.* (2010) and Martin *et al.* (2014). (1) For all the measured reference materials, the $^{18}O/^{16}O$ ratio was first corrected for IMF by reference to garnet reference material UWG2 ($\delta^{18}O$ = 5.80‰, Valley *et al.* 1995) after drift correction, if required. (2) The remaining difference between the corrected values and the laser fluorination values in the garnet reference materials is interpreted to be due to differences in the grossular, spessartine and andradite components with respect to UWG2.

Results and discussion

Major element composition of new reference materials

Crystal chemical homogeneity was tested using EPMA analyses and the results demonstrate the absence of important heterogeneities in GRS2, GRS-JH2 and CAP02 garnet materials.

GRS2 was analysed across 5 fragments of the same grain. The composition of GRS2 is $Grs_{88}Sps_1And_{10}CaTi_1$ (Table 1). The standard deviation calculated for MnO, FeO_{tot} and CaO was 0.06, 0.36 and 0.48% *m/m* respectively (2*s*). GRS-JH2 was analysed across five fragments of the same grain. The composition of GRS2 is $Grs_{83}Prp_1Sps_2And_{13}CaTi_1$ (Table 1). The standard deviation calculated for MnO, FeO_{tot}, CaO and MgO is 0.04, 0.10, 0.34 and 0.04% *m/m* respectively (2*s*). CAP02 was analysed across twenty-three grains. The composition of CAP02 is $Grs_{33}Prp_{40}Alm_{27}Sps_1$ (Table 1). The standard deviation calculated for MnO, FeO_{tot}, CaO and MgO is 0.04, 0.60, 0.96 and 1.10% *m/m* respectively (2*s*).

Oxygen isotope composition and homogeneity of new reference materials

Oxygen isotope composition of GRS2, GRS-JH2 and CAP02 was obtained by laser fluorination (LF). The homogeneity was tested by in situ measurements by SIMS across different grains or grain fragments in a way that both core and rim portions of different grain fragments were sampled. The SIMS measurements were corrected for matrix-independent instrumental mass fractionation (IMF) by using the reference material UWG2 (Appendix S1) and the uncertainty on the IMF was propagated for each individual spot analysis. The data presented in figure 2 are not corrected for matrix-effect because (1) they were used to calibrate the grossular-related matrix effect (see below) and (2) such correction(s) would apply a constant shift to the $\delta^{18}O$ value of each spot, having no effect on the spread of the analyses for each material.

Laser fluorination data for GRS2 were acquired by multiple analyses during two sessions (Table 2). The mean value of GRS2 determined by LF analysis is 8.01 ± 0.10‰ (2*s*, *n* = 4). GRS2 homogeneity was tested on five different fragments of the same grain mounted in the sample GRT-GRS (see above), for a total of seventy-nine points measured over 4 measurement sessions. Mean $\delta^{18}O$ values obtained from the four sessions are 12.58 ± 0.60‰, 11.48 ± 0.59‰, 11.30 ± 0.31‰ and 11.07 ± 0.38‰ (2*s*) (Figure 2). The repeatability of the primary reference material UWG2 during the sessions was 0.36, 0.25, 0.25 and 0.31‰ respectively. The last three sessions show results that overlap within uncertainty, while the mean result of the first session is significantly higher. The repeatability within each session is consistent and within 0.60 ‰ (2*s*), which is notably higher than that of reference material UWG2.

Laser fluorination data for GRS-JH2 were acquired by multiple analyses during one session (Table 2). The mean value of GRS-JH2 determined by LF analysis is 18.70 ± 0.08‰ (2*s*, *n* = 2). GRS-JH2 homogeneity was tested on five different grain fragments mounted in the sample GRT-GRS (see above), for a total of seventy-one points measured over four measurement sessions. Mean $\delta^{18}O$ values obtained from the four sessions were 22.64 ± 0.42‰, 22.30 ± 0.24‰, 22.71 ± 0.34‰ and 22.12 ± 0.40‰ (2*s*) (Figure 2). The repeatability of the primary reference material UWG2 during the sessions was 0.36, 0.25, 0.25 and 0.31‰ respectively. The overall mean is 22.44 ± 0.56‰ (2*s*).

Laser fluorination data for CAP02 were acquired by multiple analyses during one session (Table 2). The mean value of CAP02 determined by LF analysis is 4.64 ± 0.16‰ (2*s*, *n* = 3). CAP02 homogeneity was tested on twenty-five different grains, for total of 65 points measured over 3 measurement sessions. Mean $\delta^{18}O$ values obtained from the three sessions were 5.95 ± 0.41‰, 5.53 ± 0.46‰ and 5.67 ± 0.44‰ (2*s*) (Figure 2). The repeatability of the primary reference material UWG2 during the sessions was 0.54, 0.26 and 0.29‰ respectively. The overall mean is 5.72 ± 0.58‰ (2*s*).

Matrix effect

For this study, the measured matrix-dependent instrumental bias (matrix effect) has been correlated with the garnet end-member proportions of grossular, andradite and spessartine (Figure 3). Reference materials for spessartine and andradite were first corrected for the ubiquitous grossular effect. This is in line with the previous study by Martin *et al.* (2014) and to what done by Ickert and Stern (2013) to evaluate a possible matrix effect related to Mg content, and relies on the assumption that the grossular matrix correction remains constant despite changes in Mn and Fe in the investigated garnet samples.

To examine possible matrix effects related to Alm and Prp components, the residuals about the calibration curve for grossular were plotted against Alm, Prp and Mg# for reference materials with Sps and And < 5%, in order to minimise the effect of these components. Unlike grossular, andradite and spessartine, almandine and pyrope show no significant systematic bias and therefore no calibration curve is given for these components (Figure 4).

The repeatability of the primary reference material UWG2 over a session was between 0.24‰ and 0.48‰ (2*s*). For each curve, the mean residual (i.e., the mean of the absolute differences between the estimated values and the corresponding observed values) is reported. This value is significant (i.e., up to 0.31) and should be propagated when the final uncertainty on measurements of natural samples is calculated.

Grossular: Instrument bias correlates with the grossular content in Al-rich garnet and appears to be approximately linear for compositions of Grs = 0–35%. However, a second-degree polynomial relationship can better fit the correlation over the complete range (Figure 3a), in agreement with previous studies (e.g., Page *et al.* 2010, Martin *et al.* 2014). The similarity in the measured values in each reference material over different sessions demonstrates that the grossular component causes a bias that is reproducible over time within analytical uncertainty. The curve that fits all data points obtained across different sessions is given by the equation (R^2 = 0.97, mean residual = 0.28) (Figure 3a)

$$\text{Bias(Grs)} = -3.32\text{Grs}^2 + 8.31\text{Grs} - 1.08 \quad (1)$$

According to the measurements, the maximum bias (3.4–4.1‰) is found for reference materials with Grs = 84–86% (GRS-JH2, 10691); the bias for Grs = 88% (GRS2) is found to be slightly lower, i.e., 3.0–3.5‰. The GRS2 value obtained during the session of April 2016 shows a significantly higher bias with respect to the other sessions. This reference material was measured again for testing in August 2017 and the result is in agreement with the results obtained in December 2016 and October 2018. The polynomial predicts increasing bias from 3.4‰ to 3.7‰ with grossular content from 80% to 90%. The second-order polynomial fit reproduces within the uncertainty the measured biases for GRS-JH2, 10691 (Grs = 84–86%), while it overestimates the bias for higher grossular content. The use of two high-grossular reference materials in addition to UWG2 is strongly recommended for analysing garnet with Grs = 80–100. GRS-JH2 was analysed in different mounts over various sessions (from April 2016 to June 2019) as secondary reference material and the results have been used to test the accuracy of Equation 1 and are reported in Figure 3a.

Andradite: Measurements on andradite reference materials have first been corrected for grossular matrix effect using Equation (1). The fit of the data after correction is close to linear, but the best fit is a second-degree polynomial with equation (R^2 = 0.99, mean residual = 0.31) (Figure 3b):

$$\text{Bias(And)} = 1.85\text{And}^2 + 6.07\text{And} - 0.02 \quad (2)$$

The matrix effect increases with increasing andradite content up to 7.7‰ for And = 99% (AND-RG). The interpolated curve overestimates of ~ 0.5‰ the bias measured for And = 23% (92W2) and underestimates of ~ 0.5‰ the bias measured for And_{50} (LEW10). The correction is within the typical uncertainty of the measurements (< 0.3‰) for And = 0–5% while it becomes significant for higher andradite contents.

Spessartine: Measurements on spessartine reference materials have first been corrected for grossular matrix effect using Equation (1). The measured values in each reference material over different sessions show a variation larger than the analytical error between the first session (August 2016) and the following three sessions (August 2017, July 2018 and October 2018). This matrix effect variation can be attributed to a difference in count rates among the session of August 2016 (2.1–2.2 × 10^9 cps) and the other sessions (1.7 × 10^9 cps). Two polynomials are calculated for the session of August 2016 (Equation 3a, $R^2 > 0.99$, mean residual = 0.06) and of August 2017, July 2018 and October 2018 (Equation 3b, $R^2 = 0.91$, mean residual = 0.18):

$$\text{Bias(Sps)} = -2.21\text{Sps}^2 + 4.42\text{Sps} - 0.05 \quad (3a)$$

$$\text{Bias(Sps)} = -1.94\text{Sps}^2 + 2.87\text{Sps} - 0.03 \quad (3b)$$

For Sps < 10% a difference < 0.1‰ is observed among the two curves and the matrix effect is within the typical uncertainty of the measurements (< 0.3‰). The variation between the two different curves increases with increasing spessartine content up to > 2.0‰ for GRT-1A (Sps = 88%, Figure 3c). For this reason, it is not possible to define a unique, valid correction function. Considering the poor repeatability of spessartine related matrix effect, we recommend that at least two reference materials bracketing the composition of the unknown material should be used when measuring garnet with spessartine content above 20% to produce accurate results.

When garnets of unknown oxygen isotope composition are analysed, the precision on each analysis must take into account (1) the internal error or 'within-spot uncertainty' of the analysis, (2) the uncertainty on the primary reference material (i.e., UWG2) during the specific measurement session and (3) the uncertainty on the matrix correction(s). The final $\delta^{18}O$ value of an analysis is

$$\delta^{18}O_{final} = \delta^{18}O_{measured} - IMF - Bias \quad (4)$$

where $\delta^{18}O_{measured}$ is the row value of the analysis, with the associated internal error, IMF is the matrix-independent mass fractionation, the uncertainty of which is that on the primary reference material used for the IMF calculation, and Bias is the matrix effect for a given composition, associated to the uncertainty on the calibration. Hence, the final uncertainty on the sum is found as the sum of the uncertainties propagated in quadratic (i.e., the square root of the sum of the squared uncertainties on the single components).

Variability of matrix bias calibrations

The observed matrix effect for Grs < 50% agrees within 0.1‰ with the one described by Ickert and Stern (2013) (determined using a Cameca IMS 1280 instrument at the University of Alberta, Canada), and within 0.3‰ with the ones described by Page *et al.* (2010) (determined using a Cameca IMS 1280 multi-collector ion microprobe at the University of Wisconsin, Madison), by Martin *et al.* (2014) (determined using a SHRIMP-SI at the Australian National University) and by Raimondo *et al.* (2012) (determined using a Cameca IMS 1280 multi-collector ion microprobe at the University of Western Australia). For Grs > 50%, the observed matrix effect is up to 1‰ larger than the one described by Page *et al.* (2010), Ickert and Stern (2013) and Raimondo *et al.* (2012), and up to 3‰ larger than the one described by Martin *et al.* (2014) (Figure 3a). It is important to note that Page *et al.* (2010) and Raimondo *et al.* (2012) provide a correction based on the combination of grossular + uvarovite ($Ca_3Cr_2Si_3O_{12}$) content, but the latter never exceed 1% in the reference materials used in this study, resulting in insignificant bias. Ickert and Stern (2013) propose a correction based on Ca/(Mg+Fe^{2+}+Ca) instead of garnet end-members; in absence of Mn, Fe^{3+}, Cr^{3+} or Ti^{4+}, this corresponds to the grossular component. Hence, the matrix correction for oxygen isotope measurements in garnet due to grossular content is remarkably robust and reproducible across different instruments and laboratories up to Grs = 50%. For garnet with higher grossular content significant variations are observed in the shape and maximum value of the curve and thus individual calibrations are required with every instrument. Part of this discrepancy is possibly due to the paucity of reference material in the range Grs = 40–80 %, which would better define the shape of the curve.

The observed andradite matrix effect is close in trend and amplitude to the one reported by Martin *et al.* (2014) (Figure 3b). Page *et al.* (2010) did not treat each component separately, but the bias observed for high-And, low-Grs garnet LEW2 ($And_{91}Grs_6Alm_3$, bias = 7.1‰) is in agreement with this study (mean bias for LEW2 = 6.5‰, Table 3). Despite the andradite matrix correction being the most significant (up to ~ 8‰), no significant variation have been observed using two different instruments (Cameca 1280 vs. SHRIMP).

The observed spessartine matrix effect is shown to vary significantly over different measurement sessions on the SwissSIMS instrument and it differs from the one described by Martin *et al.* (2014) using a SHRIMP instrument (Figure 3c). This makes the matrix correction for spessartine impossible to predict within useful repeatability and demands that analyses of spessartine rich garnet be always run against multiple reference material.

No significant matrix effect associated with the almandine and pyrope components was observed (Figure 4). This result is consistent with the data of Ickert and Stern (2013). Ickert and Stern (2013) showed that the matrix effect associated with Mg in garnet is negligible for an energy window of 50 eV (i.e., that used in this study), but becomes visible by narrowing the energy window, i.e., to 20 eV.

Conclusions

Oxygen isotope measurements of three new garnet reference materials GRS2, GRS-JH2 and CAP02 are presented. The mean $\delta^{18}O$ values were characterised by laser fluorination and the homogeneity was tested with *in situ* measurements by SIMS. The mean $\delta^{18}O$ values determined by laser fluorination are GRS2 = 8.01 ± 0.10‰, GRS-JH2 = 18.70 ± 0.08‰ and CAP02 = 4.64 ± 0.16‰ (2*s*). The repeatability within each session of SIMS analyses is 0.30–0.60‰, 0.24–0.42‰ and 0.40–0.46‰ (2*s*) respectively. GRS2, GRS-JH2 and CAP02 are suitable as reference materials for SIMS analysis of grossular rich garnet.

The matrix effect for oxygen isotope analysis in garnet by Cameca IMS 1280HR at the SwissSIMS laboratory is confirmed to be correlated to the grossular, andradite and spessartine component abundance by a second-degree polynomial. Such bias can be corrected using empirically determined calibration curves, given that the relative abundance of the three end-members in the measured garnet is known. The grossular- and andradite-related matrix effects are found to be reproducible across different sessions and sample mounts, but not across instruments and laboratories for Grs > 50%. The spessartine-related matrix effect is not reproducible across different sessions or instruments. Hence, the use of two secondary reference materials that compositionally bracket the unknown sample is highly recommended in order to accurately correct the $^{18}O/^{16}O$ measurements, especially for garnet with Sps > 10% and/or Grs > 50%.

Acknowledgements

We thank Pierre Lanari for the assistance during EPMA measurement sessions and Jörg Hermann for donating garnet samples. We thank the two anonymous reviewers whose comments helped improve and clarify this manuscript. This work was supported by the Swiss National Science Foundation [Project N. 200021_166280].

References

Brouwer F.M., Burri T., Engi M. and Berger A. (2005)
Eclogite relics in the Central Alps: PT-evolution, Lu-Hf ages, and implications for formation of tectonic mélange zones. **Schweizerische Mineralogische und Petrographische Mitteilungen, 85,** 147–174.

Chamberlain C.P. and Conrad M.E. (1991)
Oxygen isotope zoning in garnet. **Science, 254,** 403–406.

Coplen T.B., Kendall C. and Hopple J. (1983)
Comparison of stable isotope reference samples. **Nature, 302,** 236–238.

Deer W., Howie R. and Zussman J. (1992)
An introduction to the rock-forming minerals. **Longman Scientific and Technology (London).**

Eiler J.M., Graham C. and Valley J.W. (1997)
SIMS analysis of oxygen isotopes: Matrix effects in complex minerals and glasses. **Chemical Geology, 138,** 221–244.

Errico J.C., Barnes J.D., Strickland A. and Valley J.W. (2013)
Oxygen isotope zoning in garnets from Franciscan eclogite blocks: Evidence for rock–buffered fluid interaction in the mantle wedge. **Contributions to Mineralogy and Petrology, 166,** 1161–1176.

Gonzaga R.G., Lowry D., Jacob D.E., LeRoex A., Schulze D. and Menzies M.A. (2010)
Eclogites and garnet pyroxenites: Similarities and differences. **Journal of Volcanology and Geothermal Research, Making and Breaking the Arc: A volume in honour of Professor John Gamble, 190,** 235–247.

Ickert R.B. and Stern R.A. (2013)
Matrix corrections and error analysis in high-precision SIMS $^{18}O/^{16}O$ measurements of Ca–Mg–Fe garnet. **Geostandards and Geoanalytical Research, 37,** 429–448.

Kita N.T., Ushikubo T., Fu B. and Valley J.W. (2009)
High precision SIMS oxygen isotope analysis and the effect of sample topography. **Chemical Geology, 264,** 43–57.

Kohn M.J. and Valley J.W. (1998)
Effects of cation substitutions in garnet and pyroxene on equilibrium oxygen isotope fractionations. **Journal of Metamorphic Geology, 16,** 625–639.

Lacroix B. and Vennemann T. (2015)
Empirical calibration of the oxygen isotope fractionation between quartz and Fe–Mg-chlorite. **Geochimica et Cosmochimica Acta, 149,** 21–31.

Martin L.A., Rubatto D., Crépisson C., Hermann J., Putlitz B. and Vitale-Brovarone A. (2014)
Garnet oxygen analysis by SHRIMP-SI: Matrix corrections and application to high-pressure metasomatic rocks from Alpine Corsica. **Chemical Geology, 374,** 25–36.

Page F.Z., Essene E.J., Mukasa S.B. and Valley J.W. (2013)
A garnet–zircon oxygen isotope record of subduction and exhumation fluids from the Franciscan Complex, California. **Journal of Petrology, 55**, 103–131.

Page F.Z., Kita N.T. and Valley J.W. (2010)
Ion microprobe analysis of oxygen isotopes in garnets of complex chemistry. **Chemical Geology, 270,** 9–19.

Peres P., Kita N.T., Valley J.W., Fernandes F. and Schuhmacher M. (2013)
New sample holder geometry for high precision isotope analyses. **Surface and Interface Analysis, 45,** 553–556.

Quinn R.J., Kitajima K., Nakashima D., Spicuzza M.J. and Valley J.W. (2017)
Oxygen isotope thermometry using quartz inclusions in garnet. **Journal of Metamorphic Geology, 35,** 231–252.

Raimondo T., Clark C., Hand M., Cliff J. and Harris C. (2012)
High-resolution geochemical record of fluid–rock interaction in a mid-crustal shear zone: A comparative study of major element and oxygen isotope transport in garnet. **Journal of Metamorphic Geology, 30,** 255–280.

Regier M., Miškovic A., Ickert R.B., Pearson D.G., Stachel T., Stern R.A. and Kopylova M. (2018)
An oxygen isotope test for the origin of Archaean mantle roots. **Geochemical Perspectives Letters, 9,** 6–10.

Riciputi L.R., Paterson B.A. and Ripperdan R.L. (1998)

Measurement of light stable isotope ratios by SIMS: Matrix effects for oxygen, carbon, and sulfur isotopes in minerals. **International Journal of Mass Spectrometry, 178,** 81–112.

Rubatto D. and Angiboust S. (2015)
Oxygen isotope record of oceanic and high-pressure metasomatism: a P–T–time–fluid path for the Monviso eclogites (Italy). **Contributions to Mineralogy and Petrology, 170,** 44.

Seitz S., Baumgartner L.P., Bouvier A.-S., Putlitz B. and Vennemann T. (2017)
Quartz reference materials for oxygen isotope analysis by SIMS. **Geostandards and Geoanalytical Research, 41,** 69–75.

Sharp Z.D. (1990)
A laser-based microanalytical method for the in situ determination of oxygen isotope ratios of silicates and oxides. **Geochimica et Cosmochimica Acta, 54,** 1353–1357.

Shimura T. and Kemp A.I.S. (2015)
Tetrahedral plot diagram: A geometrical solution for quaternary systems. **American Mineralogist, 100,** 2545–2547.

Urosevic M., Nebel O., Padrón-Navarta J.A. and Rubatto D. (2018)
Assessment of O and Fe isotope heterogeneity in garnet from Kakanui (New Zealand) and Erongo (Namibia). **European Journal of Mineralogy, 30,** 695–710.

Valley J.W., Kitchen N., Kohn M.J., Niendorf C.R. and Spicuzza M.J. (1995)
UWG-2, a garnet standard for oxygen isotope ratios: strategies for high precision and accuracy with laser heating. **Geochimica et Cosmochimica Acta, 59,** 5223–5231.

Vielzeuf D., Champenois M., Valley J.W., Brunet F. and Devidal J.L. (2005a)
SIMS analyses of oxygen isotopes: Matrix effects in Fe–Mg–Ca garnets. **Chemical Geology, 223,** 208–226.

Vielzeuf D., Veschambre M. and Brunet F. (2005b)

Oxygen isotope heterogeneities and diffusion profile in composite metamorphic-magmatic garnets from the Pyrenees. **American Mineralogist, 90,** 463–472.

Supporting information

The following supporting information may be found in the online version of this article:

Appendix S1. All measurement results.

This material is available from:
http://onlinelibrary.wiley.com/doi/10.1111/ggr.00000/abstract
(This link will take you to the article abstract).

Figure captions

Figure 1. Tetrahedral plot (constructed with the Excel spreadsheet by Shimura and Kemp 2015) showing the composition of reference garnet samples used in this study. Stars represent the reference materials characterised in this study; dots represent garnet samples characterised in previous studies (see text for details). Symbol fill colours show for which calibration (i.e., grossular, andradite or spessartine matrix effect correction) each of the material was used.

Figure 2. $\delta^{18}O$ SIMS values for (a) CAP02, (b) GRS2 and (c) GRS-JH2. The data were corrected for IMF using UWG2 garnet as primary reference material. The uncertainty shown for a single analysis (2*s*) combines the measurement standard error and the uncertainty on the matrix-independent IMF. Mean values for each measurement session are reported (grey lines) with standard deviations (2*s*) for each session (shaded bands).

Figure 3. Matrix effect plotted as a function of garnet end-member proportion for (a) grossular, (b) andradite and (c) spessartine. Vertical bars represent the standard errors combined with the uncertainty on the IMF (± 2*s*). The solid lines are best-fit regressions through the measurements from this study; dashed lines are regressions from Page *et al.* (2010) (P10), Raimondo *et al.* (2012) (R12), Ickert and Stern (2013) (IS13) and Martin *et al.* (2014) (M14). Data marked as "TEST" were not used for the regression, but they were used as independent constraints to test the validity of the calculated functions. Data shown in panels (b) and (c) were first corrected for any grossular effect.

Figure 4. Testing the matrix effect of Fe and Mg content. The matrix bias ($\delta^{18}O_{SIMS} - \delta^{18}O_{LF}$) after the Grs correction for each sample and session are plotted against (a) Alm, (b) Prp and (c) Mg#. Only garnet reference materials with And < 10% and Sps < 5% were considered. Vertical bars represent the standard errors combined with the uncertainty on the IMF (± 2*s*). No significant correlation was observed.

Table 1.

Major element composition of the garnet samples GRS2 (number of analyses = 52), GRS-JH2 (number of analyses = 50) and CAP02 (number of analyses = 139)

	GRS2		**GRS-JH2**		**CAP02**	
	Mean oxide % *m/m*	**2*s***	**Mean oxide % *m/m***	**2*s***	**Mean oxide % *m/m***	**2*s***
SiO_2	38.32	0.46	39.00	0.34	40.71	0.62
Al_2O_3	20.73	0.76	19.38	0.30	22.79	0.44
TiO_2	0.20	0.08	0.41	0.08	0.07	0.04
MgO	0.06	0.04	0.14	0.04	10.81	1.10
FeO	2.99	0.36	4.41	0.10	13.24	0.60
MnO	0.24	0.06	0.77	0.04	0.27	0.04
CaO	36.86	0.48	35.83	0.34	12.37	0.96
Cr_2O_3	0.01	0.02	0.01	0.02	na	na
Total	99.41	0.96	99.94	0.54	100.27	1.74
	Cations, charge balance		**Cations, charge balance**		**Cations, charge balance**	
Si	2.91		2.97		3.01	
Al^{VI}	1.86		1.74		1.98	
Ti	0.01		0.02		0.00	
Fe^{3+}	0.19		0.28		0.02	
Fe^{2+}	0.00		0.01		0.80	
Mn	0.02		0.05		0.02	
Mg	0.01		0.02		1.19	
Ca	3.00		2.92		0.98	
	End member (%)	**2*s***	**End member (%)**	**2*s***	**End member (%)**	**2*s***
Alm	0.00	0.00	0.43	0.96	26.87	1.56
Prp	0.22	0.18	0.54	0.12	39.79	3.02
Grs	88.33	1.28	83.31	0.70	32.46	2.92
Sps	0.53	0.16	1.65	0.08	0.57	0.10
And	10.37	1.08	12.94	1.54	0.24	0.60
Ca-Ti	0.55	0.24	1.14	0.20	0.06	0.04

Table 2.

Oxygen isotope composition of garnet samples GRS2, GRS-JH2 and CAP02 determined by CO_2 laser fluorination analysis

	$\delta^{18}O$ (‰) corrected	Reference material	$\delta^{18}O$ raw (‰)*
GRS2			
Session 03.07.2012			
analysis 1	8.08	NBS-28 quartz	9.39 ± 0.10 (*n* = 4) (2*s*)
analysis 2	8.03		
Mean session 1	8.05 ± 0.06 (2*s*)		
Session 11.07.2012			
analysis 3	8.00	NBS-28 quartz	9.42 ± 0.45 (*n* = 6) (2*s*)
analysis 4	7.96		
Mean session 2	7.98 ± 0.06 (2*s*)		
Mean GRS2	*8.01 ± 0.10 (2s)*		
GRS-JH2			
Session 21.02.2017			
analysis 1	18.73	NBS-28 quartz	9.66 ± 0.04 (*n* = 4) (2*s*)
analysis 2	18.68		
Mean GRS-JH2	*18.70 ± 0.08 (2s)*		
CAP02			
Session 13.06.2019			
analysis 1	4.73	NBS-28 quartz	9.36 ± 0.30 (*n* = 3) (2*s*)
analysis 2	4.58		
analysis 3	4.62		
Mean CAP02	*4.64 ± 0.16 (2s)*		

*The mean of all NBS-28 quartz reference material analyses for these four sessions between 2012 and 2019 was 9.46 ± 0.34 ‰ (2*s*).

Table 3.

Summary of analytical data from garnet reference materials. Data are organized as follows: (1) reference materials used in the grossular correction; (2) reference materials used in the andradite correction; (3) reference materials used in the spessartine correction and (4) reference materials measured as tests (i.e., not used for the regressions). Within each block, UWG2 is reported as first and the other garnet samples follow in order of increasing grossular. For all the test measurements UWG2 was used as primary reference material to correct for the matrix independent IMF but it is not reported. The uncertainty on the IMF corrected $\delta^{18}O_{SIMS}$ (2s) accounts for (1) the uncertainty on the mean and (2) that on the IMF calculation

Garnet name	**Composition**	**Mount**	**Session**	**$\delta^{18}O_{SIMS}$ (IMF corr.)**	**2s abs.* (N. of measurements)**	**$\delta^{18}O_{LF}$**	**Bias**	**Bias (Grs corr.)**
Reference materials used in the grossular correction								
UWG2	$Grs_{14}Prp_{40}Alm_{45}Sps_{1}And_{0}$	GRT-GRS	April 2016 (1)	5.80	0.36 (9)	5.80[a]	-	-
		GRT-GRS	April 2016 (2)	5.80	0.48 (75)		-	-
		GRT-GRS	December 2016	5.80	0.40 (29)		-	-
		CAP02	March 2018	5.80	0.54 (18)		-	-
		GRT-GRS	October 2018	5.80	0.31 (47)		-	-
		CAP02	October 2018	5.80	0.26 (9)		-	-
		CAP02	June 2019	5.80	0.29 (12)		-	-
B114	$Grs_{6}Prp_{31}Alm_{61}Sps_{2}And_{0}$	GRT-GRS	April 2016 (1)	8.57	0.52 (10)	9.30[b]	-0.73	-
		GRT-GRS	April 2016 (2)	8.82	0.68 (10)		-0.48	-
		GRT-GRS	December 2016	8.49	0.60 (11)		-0.81	-
		GRT-GRS	October 2018	8.54	0.47 (12)		-0.76	-
PRPAA	$Grs_{11}Prp_{69}Alm_{18}Sps_{1}And_{0}Uv_{1}$	GRT-GRS	April 2016 (2)	5.62	0.62 (25)	5.50 [b]	0.12	-
		GRT-GRS	December 2016	5.84	0.50 (12)		0.34	-
		GRT-GRS	October 2018	5.59	0.42 (12)		0.09	-
PRPAK	$Grs_{11}Prp_{64}Alm_{24}Sps_{1}And_{0}$	GRT-GRS	April 2016 (2)	5.28	0.64 (24)	5.50 [b]	-0.22	-
		GRT-GRS	December 2016	5.70	0.49 (12)		0.20	-
		GRT-GRS	October 2018	5.46	0.47 (12)		-0.04	-
Kakanui	$Grs_{13}Prp_{60}Alm_{25}Sps_{1}And_{0}$	GRT-GRS	April 2016 (2)	5.59	0.60 (25)	5.22 [c]	0.24	-
		GRT-GRS	December 2016	5.79	0.49 (12)		0.29	-
		GRT-GRS	October 2018	5.35	0.45 (11)		0.00	-

2B3	$Grs_{24}Prp_{3}Alm_{67}Sps_{4}And_{2}$	GRT-GRS	April 2016 (2)	7.96	0.72 (20)	6.90 [b]	1.06	-
		GRT-GRS	December 2016	7.89	0.61 (9)		0.99	-
		GRT-GRS	October 2018	7.66	0.37 (9)		0.76	-
CAP02	$Grs_{32}Prp_{40}Alm_{27}Sps_{1}And_{0}$	CAP02	March 2018	5.95	0.68 (23)	4.64 [g]	1.31	-
		CAP02	October 2018	5.56	0.44 (20)		0.92	-
		CAP02	June 2019	5.71	0.48 (19)		1.07	-
GRS-JH2	$Grs_{83}Prp_{1}Alm_{0}Sps_{2}And_{13}CaTi_{1}$	GRT-GRS	April 2016 (2)	22.64	0.64 (23)	18.70 [g]	3.94	-
		GRT-GRS	December 2016	22.62	0.53 (12)		3.92	-
		GRT-GRS	October 2018	22.09	0.51 (12)		3.39	-
10691	$Grs_{86}Prp_{2}Alm_{5}Sps_{0}And_{5}CaTi_{2}$	GRT-GRS	April 2016 (2)	3.60	0.98 (24)	0.18 [b]	3.42	-
		GRT-GRS	December 2016	3.90	0.50 (12)		3.72	-
		GRT-GRS	October 2018	3.48	0.40 (9)		3.30	-
GRS2	$Grs_{88}Prp_{0}Alm_{0}Sps_{1}And_{10}CaTi_{1}$	GRT-GRS	April 2016 (2)	12.61	0.72 (24)	8.01 [g]	4.60	-
		GRT-GRS	December 2016	11.25	0.51 (18)		3.24	-
		GRT-GRS	October 2018	11.04	0.49 (12)		3.03	-
Reference materials used in the andradite correction								
UWG2	$Grs_{14}Prp_{40}Alm_{45}Sps_{1}And_{0}$	GRT-AND	March 2017	5.80	0.31 (40)	5.80 [a]	-	-
		GRT-AND	June 2019	5.80	0.41 (26)		-	-
AndRG	$Grs_{0}Prp_{0}Alm_{1}Sps_{0}And_{99}$	GRT-AND	March 2017	11.02	0.43 (18)	4.39 [d]	6.63	7.71
		GRT-AND	June 2019	10.99	0.57 (12)		6.60	7.68
LEW2	$Grs_{6}Prp_{0}Alm_{3}Sps_{0}And_{91}$	GRT-AND	March 2017	4.94	0.43 (18)	-1.47 [b]	6.41	7.00
		GRT-AND	June 2019	5.01	0.53 (11)		6.48	7.07
2B3	$Grs_{24}Prp_{3}Alm_{67}Sps_{4}And_{2}$	GRT-AND	March 2017	7.83	0.42 (11)	6.90 [b]	0.93	0.19
		GRT-AND	June 2019	7.76	0.64 (9)		0.86	0.12
LEW10	$Grs_{42}Prp_{2}Alm_{4}Sps_{0}And_{50}CaTi_{2}$	GRT-AND	March 2017	4.63	0.43 (17)	-1.20 [b]	5.83	3.99
		GRT-AND	June 2019	4.75	0.54 (12)		5.95	4.11
92-W2	$Grs_{72}Prp_{1}Alm_{4}Sps_{0}And_{23}$	GRT-AND	March 2017	4.91	0.52 (17)	0.81 [e]	4.10	0.92
		GRT-AND	June 2019	4.63	0.54 (12)		3.82	0.64
10691	$Grs_{86}Prp_{2}Alm_{5}Sps_{0}And_{5}CaTi_{2}$	GRT-AND	March 2017	3.65	0.37 (11)	0.18 [b]	3.47	-0.12
		GRT-AND	June 2019	3.63	0.71 (9)		3.45	-0.14

Reference materials used in the spessartine correction								
UWG2	$Grs_{14}Prp_{40}Alm_{45}Sps_{1}And_{0}$	GRT-SPS	August 2016 (1)	5.80	0.11 (13)	5.80 [a]	-	-
		GRT-SPS	August 2016 (2)	5.80	0.19 (18)		-	-
		GRT-SPS	August 2016 (3)	5.80	0.35 (16)		-	-
		GRT-SPS	August 2017 (1)	5.80	0.24 (14)		-	-
		GRT-SPS	August 2017 (2)	5.80	0.25 (13)		-	-
		GRT-SPS	July 2018	5.80	0.22 (31)		-	-
		GRT-SPS	October 2018 (1)	5.80	0.21 (18)		-	-
		GRT-SPS	October 2018 (2)	5.80	0.22 (14)		-	-
GRT1A	$Grs_{1}Prp_{1}Alm_{10}Sps_{88}And_{0}$	GRT-SPS	August 2016 (3)	11.21	0.42 (23)	10.12 [d]	1.09	2.09
		GRT-SPS	August 2017 (2)	10.00	0.28 (13)		-0.12	0.88
		GRT-SPS	July 2018	10.33	0.35 (12)		0.21	1.20
		GRT-SPS	October 2018 (1)	9.93	0.40 (12)		-0.19	0.80
ErrRED	$Grs_{2}Prp_{3}Alm_{67}Sps_{28}And_{0}$	GRT-SPS	August 2016 (2)	9.35	0.52 (24)	9.30 [f]	0.05	0.96
		GRT-SPS	August 2017 (1)	8.93	0.48 (18)		-0.37	0.54
		GRT-SPS	July 2018	9.34	0.35 (12)		0.04	0.95
		GRT-SPS	October 2018 (2)	8.61	0.46(12)		-0.69	0.23
SPEBH	$Grs_{7}Prp_{1}Alm_{22}Sps_{68}And_{1}$	GRT-SPS	August 2016 (3)	9.63	0.56 (23)	8.13 [d]	1.50	2.01
		GRT-SPS	August 2017 (2)	8.73	0.33 (14)		0.60	1.11
		GRT-SPS	July 2018	8.86	0.32 (12)		0.73	1.24
		GRT-SPS	October 2018 (1)	8.51	0.45 (12)		0.38	0.89
2B3	$Grs_{24}Prp_{3}Alm_{67}Sps_{4}And_{2}$	GRT-SPS	August 2016 (1)	7.68	0.39 (19)	6.90 [b]	0.78	0.04
		GRT-SPS	August 2017 (1)	7.86	0.51 (15)		0.96	0.22
		GRT-SPS	July 2018	7.83	0.39 (12)		0.93	0.19
		GRT-SPS	October 2018 (2)	7.42	0.63 (9)		0.52	-0.21
*Reference materials measured as test** and as secondary standard during various sessions in the period April 2016 – June 2019 (in addition to UWG2)*								
ErrRED	$Grs_{2}Prp_{3}Alm_{67}Sps_{28}And_{0}$	GRT-SPS	December 2016	9.25	0.59 (10)	9.30 [f]	-0.05	0.86
2B3	$Grs_{24}Prp_{3}Alm_{67}Sps_{4}And_{2}$	GRT-AND	December 2016 (1)	7.67	0.55 (9)	6.90 [b]	0.77	0.03
		GRT-SPS	December 2016 (2)	7.73	0.48 (9)		0.83	0.09
GRS-JH2	$Grs_{83}Prp_{1}Alm_{0}Sps_{2}And_{13}CaTi_{1}$	GRT-GRS	August 2016	22.30	0.33 (23)	18.70 [g]	3.60	-

		other	December 2016	22.40	0.48 (11)		3.70	-
		other	March 2017	22.32	0.61 (9)		3.62	-
		other	November 2017 (1)	22.20	0.46 (4)		3.50	-
		other	November 2017 (2)	22.80	0.31 (5)		4.10	-
		other	January 2018 (1)	22.40	0.34 (10)		3.70	-
		other	January 2018 (2)	22.26	0.29 (13)		3.56	-
		other	July 2018	21.94	0.35 (8)		3.24	-
		other	June 2019 (1)	21.91	0.70 (4)		3.21	-
		other	June 2019 (2)	22.07	0.59 (8)		3.37	-
10691	$Grs_{86}Prp_{2}Alm_{5}Sps_{0}And_{5}CaTi_{2}$	GRT-AND	December 2016	3.72	0.39 (10)	0.18 [b]	3.54	-0.05
GRS2	Grs_{88} $Prp_{0}Alm_{0}Sps_{1}And_{10}CaTi_{1}$	GRT-GRS	August 2016	11.48	0.65 (24)	8.01 [g]	3.47	-

* For reference materials other than UWG2, the uncertainty on the IMF was propagated. When two or three distinct blocks were analysed within the same session, they are numbered as (1), (2) and (3).

** Data not used for the regressions.

[a] Valley *et al.* (1995).

[b] As reported in Page *et al.* (2010).

[c] Gonzaga *et al.* (2010).

[d] Martin *et al.* (2014)

[e] As reported in Martin *et al.* (2014)

[f] Urosevic *et al.* (2018)

[g] This study.

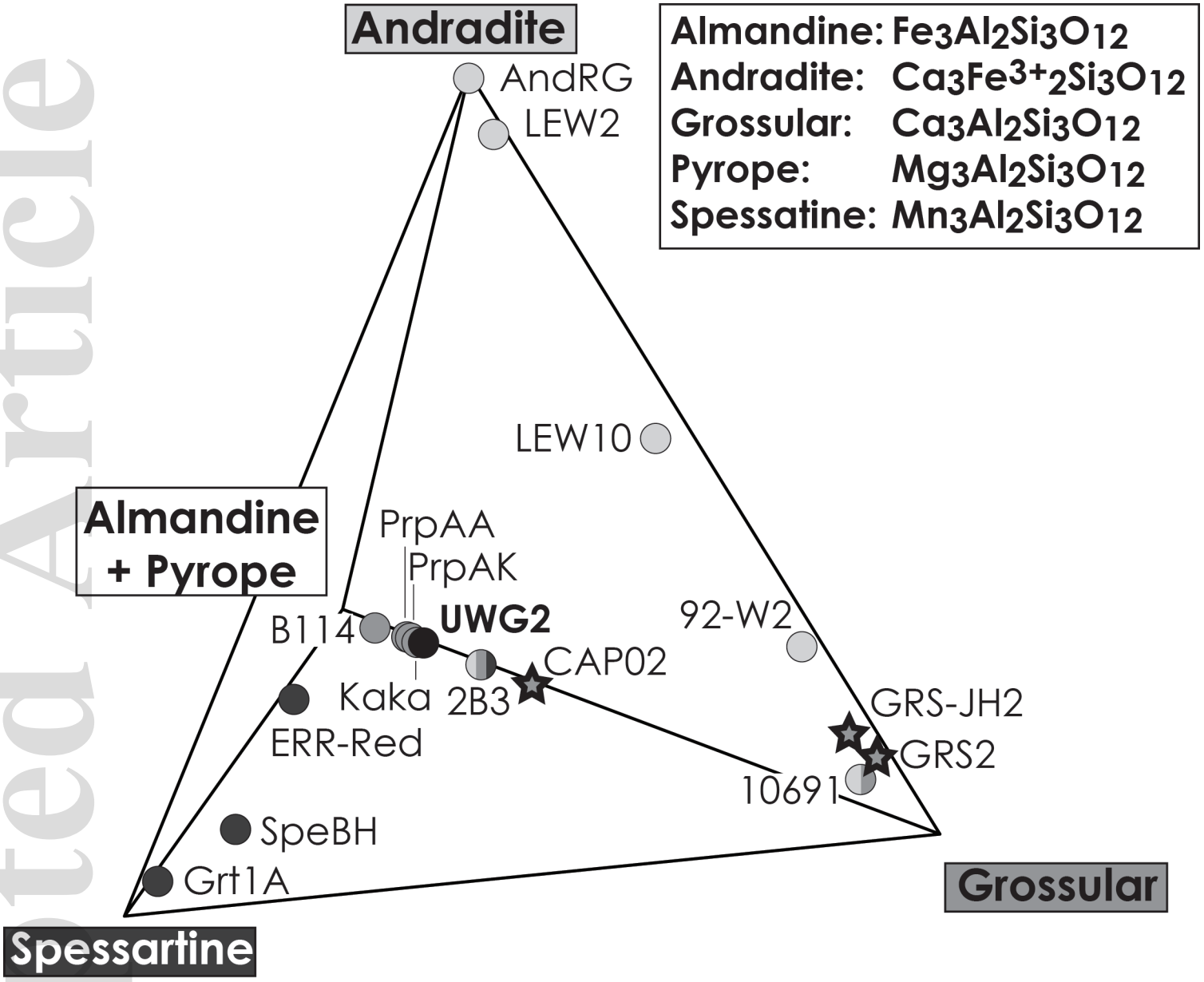

ggr_12324_f1.tif

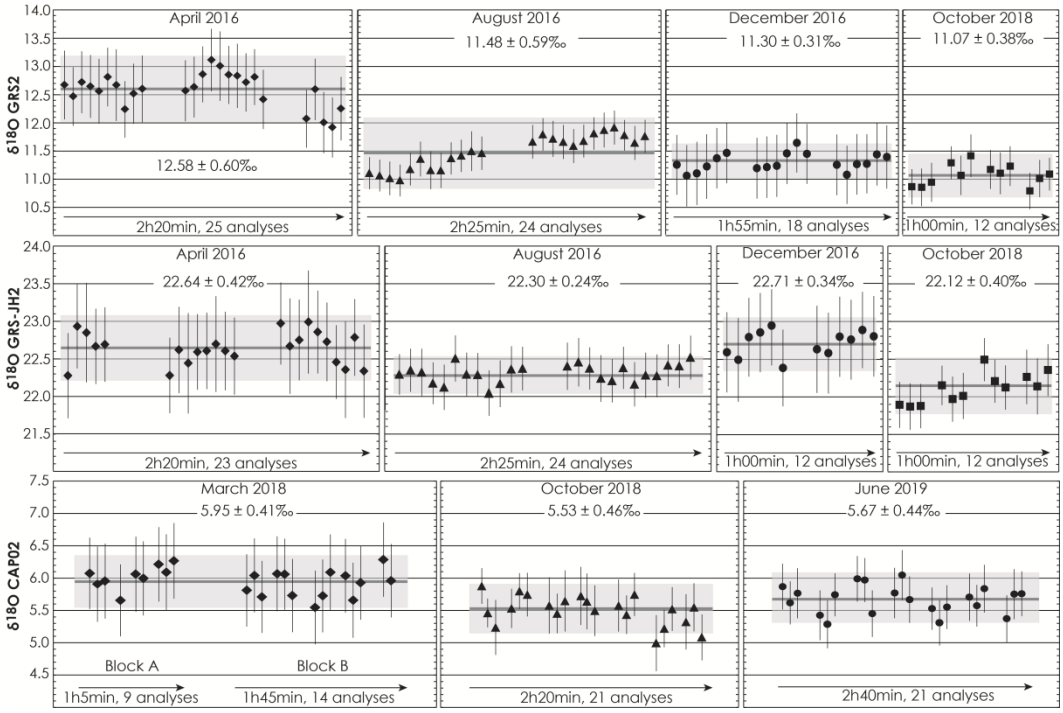

ggr_12324_f2.tif